Deep Transfer Learning-Based Sizing Method of Permanent Magnet Synchronous Motors Considering Axial Leakage Flux

Soo-Hwan Park[1], Jun-Woo Chin[2], Kyoung-Soo Cha[1], and Myung-Seop Lim[1]

[1]Department of Automotive Engineering, Hanyang University, Seoul 04763, Republic of Korea
[2]Advanced Powertrain Research and Development Center, Korea Automotive Technology Institute, Cheonan 31214, Republic of Korea

The sizing process is necessary to analyze the electromagnetic characteristics according to the major shape parameters during the early design stage of permanent magnet synchronous motors (PMSMs). However, predicting the performance of PMSMs with 2-D finite element analysis (FEA) has errors due to axial leakage flux. Therefore, the axial leakage flux should be considered in the sizing process. The most accurate way to consider the axial leakage flux is to perform 3-D FEA, but it has a disadvantage of high computational cost. In this view, we propose a deep transfer learning-based surrogate modeling method to reduce the computational cost for calculating 3-D FEA-based motor parameters. The transfer learning is conducted using a large amount of 2-D FEA-based and small amount of 3-D FEA-based motor parameters. Using the proposed process, it is possible to accurately predict the motor characteristics according to size-related variables that satisfy the required specifications with small amount of 3-D FEA-based motor parameters. The proposed method was verified through 3-D FEA and experiments for pancake-type PMSMs, which is highly affected by axial leakage flux.

Index Terms—**Deep neural network (DNN), permanent magnet synchronous motors (PMSMs), shape ratio, split ratio, torque per rotor volume (TRV), transfer learning.**

I. Introduction

PERMANENT magnet synchronous machines (PMSMs) are mainly used as servo motors that require precise control due to their electromagnetic characteristics such as high power density, low torque ripple, and cogging torque [1]. Manufacturers of the servo motor develop various models by changing winding specifications and axial length using the same stator and rotor core because of cost reduction and quality control. In addition, the manufacturers develop motors with high or low output power by changing the outer diameter of motor based on the previously developed motors. In other words, a sizing method which controls shape ratio and split ratio is important in servo motors [2], [3].

The size of PMSMs can be determined using size-related variables such as torque per rotor volume (TRV), shape ratio, and split ratio which are related to the magnetic circuit of the motors [2]. The shape ratio is defined as the ratio of the axial length to the rotor outer diameter, and the split ratio is defined as the ratio of the rotor outer diameter to the stator outer diameter. Therefore, the electromagnetic characteristics of PMSMs are highly affected by size-related variables.

Since the main flux path of PMSMs is orthogonal to the rotation axis of the rotor, an electromagnetic analysis is usually conducted by modeling the magnetic circuit as a 2-D cross section. However, there exists leakage flux in the axial direction that does not pass through the airgap. Since leakage flux causes a decrease in electromagnetic torque, it should be considered for accurate estimation of electromagnetic characteristics. Especially, it is important to consider axial leakage flux in the sizing process because the influence of axial leakage flux is relatively large for a pancake-type motor with a small shape ratio [4].

Therefore, we propose a computationally efficient sizing process of PMSMs using deep transfer learning. The method can be achieved by using a large amount of 2-D finite element analysis (FEA) data with low computation cost and a small amount of 3-D FEA data with high computation cost. In this article, the analysis was performed using a surface-mounted permanent magnet type rotor with overhang.

Manuscript received 28 January 2022; revised 13 April 2022; accepted 1 June 2022. Date of publication 9 June 2022; date of current version 26 August 2022. Corresponding author: M.-S. Lim (e-mail: myungseop@hanyang.ac.kr).

Color versions of one or more figures in this article are available at https://doi.org/10.1109/TMAG.2022.3181804.

Digital Object Identifier 10.1109/TMAG.2022.3181804

II. Sizing Process Based on Deep Transfer Learning

A. Sizing of PMSMs

The purpose of the sizing process is for predicting electromagnetic performance according to major geometries such as stator outer diameter and axial length of PMSMs. The electromagnetic performance is determined by materials and geometry variables which determined the electric and magnetic circuit parameters, and the geometry variables can be calculated using the size-related variables such as TRV, shape ratio, α_{shape}, and split ratio, α_{split}, defined as follows:

$$\text{TRV} = \frac{4}{\pi}\frac{T_{\text{pk}}}{D_{\text{ro}}^2 L_{\text{stk}}} \quad \alpha_{\text{shape}} = \frac{L_{\text{stk}}}{D_{\text{ro}}} \quad \alpha_{\text{split}} = \frac{D_{\text{ro}}}{D_{\text{so}}} \tag{1}$$

where T_{pk} is the peak torque, D_{so} and D_{ro} are the outer diameter of the stator and the rotor, respectively, and L_{stk} is the axial length. Therefore, the size of PMSMs can be determined by size-related variables as shown in Fig. 1. When the peak torque is constant, the rotor volume is inversely proportional to

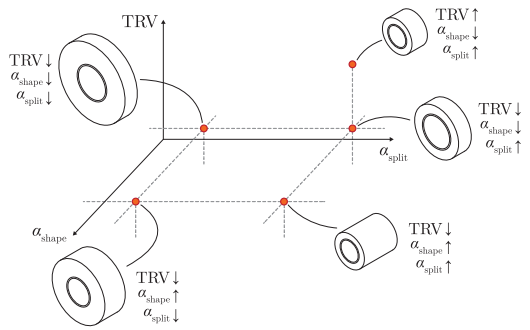

Fig. 1. Various sizes of PMSMs according to size-related variables.

TABLE I
SPECIFICATIONS AND DESIGN RANGE OF PMSM

Item	Unit	Value
Motor type	-	SPMSM
Number of poles / slots	-	20 / 18
Permanent magnets	-	N38UH
Stator/rotor core	-	35PN230
Peak torque range	Nm	5 to 20
TRV range	Nm/mm^3	55,000 to 120,000
α_{shape} range	-	0.30 to 1.20
α_{split} range	-	0.55 to 0.65

the TRV. If the volume of the motor is constant, the smaller the shape ratio, the flatter the shape of the motor and it is heavily influenced by axial leakage flux than the motor with large shape ratio. When the split ratio is increased when the stator outer diameter is constant, the space occupied by the stator core decreases and it highly causes magnetic saturation in stator core.

Table I shows the specifications and design range of PMSMs. The type of target PMSM is surface-mounted PMSM, and it has 20 poles and 18 slots. The design range of peak torque, TRV, α_{shape}, and α_{split} are listed in the table. The ratio of the tooth to the yoke of the stator, pole arc of the permanent magnets, and airgap length are set to be constant.

In this article, 2-D/3-D FEA is conducted for quantifying axial leakage flux. Since the magnetic circuit for the axial direction is considered in 3-D FEA, the axial leakage flux can be quantified using the difference in motor parameters calculated by 2-D and 3-D FEAs. Fig. 2(a) and (b) shows the comparison of 2-D and 3-D FEA-based flux linkage according to the shape ratio. In the case of small shape ratio, the ratio of permeance for the axial leakage flux to the permeance for the main flux is larger than when the shape ratio is large. Therefore, it is necessary to consider the effect of axial leakage flux in the sizing process.

B. Deep Transfer Learning

A deep neural network (DNN) is widely used as a surrogate model for optimization because it shows excellent performance on various tasks such as regression or classification [5], [6]. Generally, a large amount of data is required to achieve high performance of DNN. Therefore, applications such as regression of electromagnetic performance using 3-D FEA require a lot of computing resources to obtain high performance of DNN.

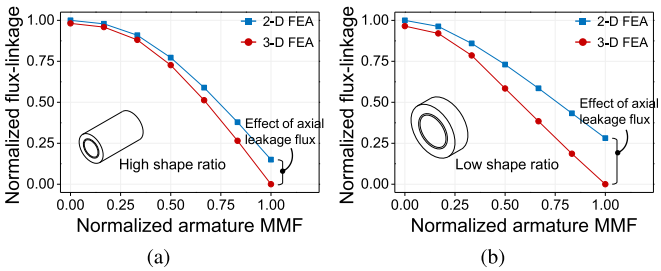

Fig. 2. Comparison of 2-D and 3-D FEA-based flux linkage according to armature current. (a) $\alpha_{\text{shape}} = 1.5$. (b) $\alpha_{\text{shape}} = 0.3$.

Transfer learning is a technique that takes domain knowledge of a pre-trained model for the multi dimensional source dataset, $\mathbf{X}^s \in \mathbf{R}^{n\times p}$, and used it to train a new model for the target dataset, $\mathbf{X}^t \in \mathbf{R}^{n\times p}$, with n denoting the number of observations and p denoting the number of input features [7]. It can be effectively used when DNN cannot be trained sufficiently because it is difficult to obtain the label of the target dataset.

The principle of transfer learning is as follows. Assume that the source and target datasets have similar distributions but have bias. The source dataset has a relatively large size compared with the target dataset because it is relatively easy to obtain labels compared with the target dataset. The source DNN has high regression performance because it is trained to follow the data distribution of the source dataset. Therefore, to use the domain knowledge of the source model that has a similar distribution to the target dataset, the layers of the target DNN except for several top layers are transferred from the pre-trained layers of the source model.

C. Proposed Sizing Process

Fig. 3 shows a flowchart for the proposed deep transfer learning-based sizing process. The 2-D FEA-based motor parameters can be acquired faster than 3-D FEA-based motor parameters, and each motor parameter has a similar data distribution. Therefore, DNNs are trained by transfer learning using 2-D FEA-based dataset as a source data and the 3-D FEA-based dataset as a target data for considering axial leakage flux. After training DNNs, the motor parameters according to the desired size-related parameters are predicted through DNNs, and the motor characteristics are calculated by conducting current vector control under given constraints.

The source and target data were labeled using JMAG, a commercial FEA software, after design of experiments based on Latin hypercube sampling. The features and design range are same as presented in Table I. For each sample, the labeling process was conducted by calculating the *d, q*-axis inductance (L_d, L_q), flux-linkage (ψ_a), and iron loss (W_i) according to the current vector and rotational speed. The *d, q*-axis inductance

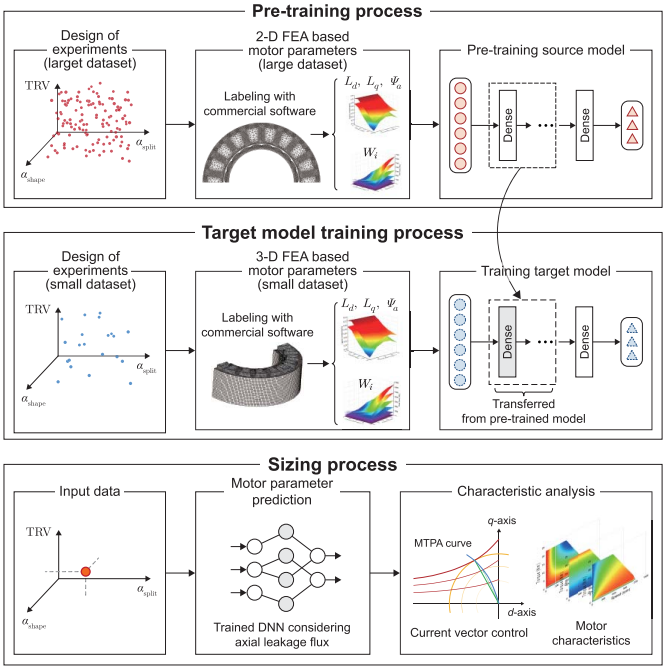

Fig. 3. Proposed deep transfer learning-based sizing process.

can be computed as

$$L_d = \frac{\psi_{od} - \psi_a}{i_{od}} \, L_q = \frac{\psi_{oq}}{i_{oq}} \tag{2}$$

where $\psi_{od,oq}$ and ψ_a are the d, q-axis flux linkage and no-load flux linkage, respectively, and $i_{od,oq}$ is the d, q-axis magnetization current. The iron loss can be calculated according to the current vector and rotational speed using material data [8].

In this article, the DNNs are divided into two types according to the attribute of the data. The first DNN is for predicting L_d, L_q, and ψ_a which are affected by magnetic saturation. It receives sizing-related parameters and current vector as input features. The second DNN is for predicting W_i which is affected by frequency and magnetic saturation. Therefore, it receives the rotational speed along with the aforementioned input features. In addition, the analysis was performed by modeling an air dummy corresponding to 50% of the axial length to consider the axial leakage path in the modeling for 3-D FEA.

D. Learning Performance With Transfer Learning

The structure of DNN was determined through the hyperparameter tuning process. The hyperparameters are tunable parameters that allow us to control the training process of deep learning model. As the performance of the model is highly dependent on the combination of hyperparameters, the process for hyperparameter tuning is necessary. The architecture of DNN was selected as a multi-layer perceptron (MLP). The perceptron is an algorithm that mimics the principle of biological neuron, which gives the sum of multiple inputs multiplied by weights. MLP is a structure in which layers, a set of perceptrons, are stacked and is generally used for pattern recognition of complex dataset. The detailed setting of DNN and the number of the source and target datasets are listed in Table II. The number of the source dataset was 33 times larger than that of the target datasets. The hyperparameters of DNN were selected as the number of hidden layers and units, and the learning rate for Adam optimizer. The hyperparameter tuning was conducted using Bayesian optimization [9] with source dataset. To avoid overfitting, the source dataset was split into training, validation, and test datasets at a ratio of 8:1:1. As a result of hyperparameter tuning, the number of layers, units, and learning rate were selected as 4, 256, and 1e-5, respectively.

TABLE II
DETAILED SETTING OF DNN AND NUMBER OF DATASET

Input features	T_{pk}, TRV, α_{shape}, α_{split}			
Output features	L_d, L_q, ψ_a		W_i	
Number of layers	4		4	
Number of units	256		256	
Learning rate	1e-5		1e-5	
Activation function	ReLU		ReLU	
Optimizer	Adam		Adam	
Loss function	Mean squared error		Mean squared error	
Size of mini-batch	16		32	
Number of dataset	9,800 (Source, 2-D)	294 (Target, 3-D)	68,600 (Source, 2-D)	2,058 (Target, 3-D)

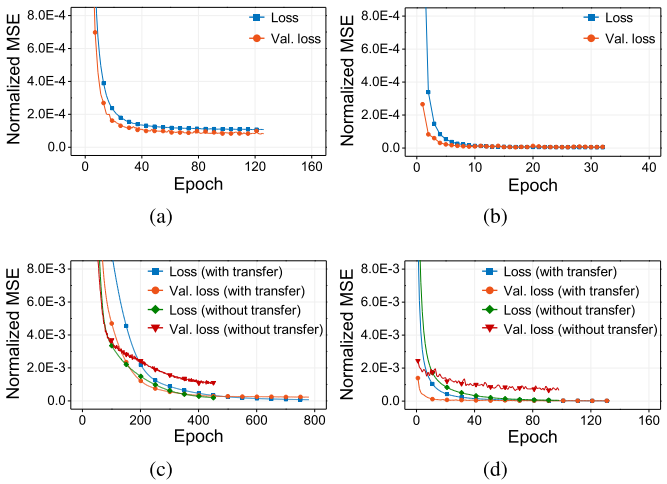

Fig. 4. Learning curve of source and target DNNs. (a) Source DNN for predicting L_d, L_q and ψ_a, (b) for predicting W_i, (c) target DNN for predicting L_d, L_q and ψ_a, and (d) for predicting W_i with or without transfer learning.

The target DNNs were trained using transfer learning, and training was conducted by transferring the weights of three layers among the four hidden layers. The target dataset was split into training and validation datasets at a ratio of 5:1, and the effect of transfer learning was verified by labeling additional test datasets with a size of 490 for predicting L_d, L_q and ψ_a and 3430 for predicting W_i.

The learning curves of the source DNNs and target DNNs with or without transfer learning are shown in Fig. 4(a)–(d). As the size of the source dataset was large enough, it can be seen that the normalized mean squared error (MSE) of source

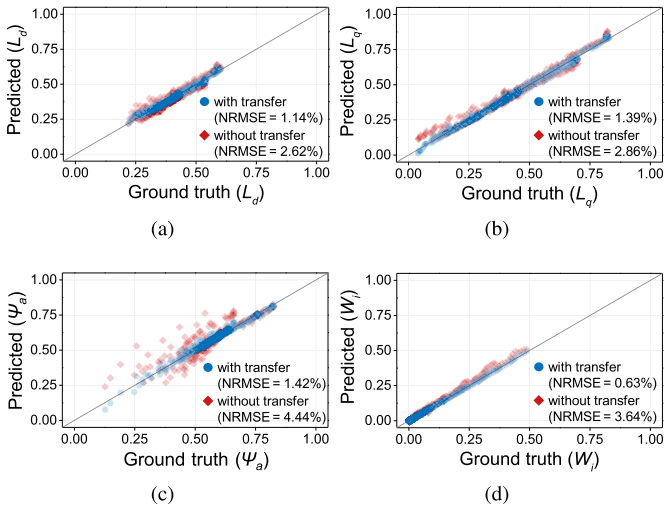

Fig. 5. Comparison between ground truth and prediction with or without transfer learning for test dataset. Results of comparing (a) L_d, (b) L_q, (c) ψ_a, and (d) W_i.

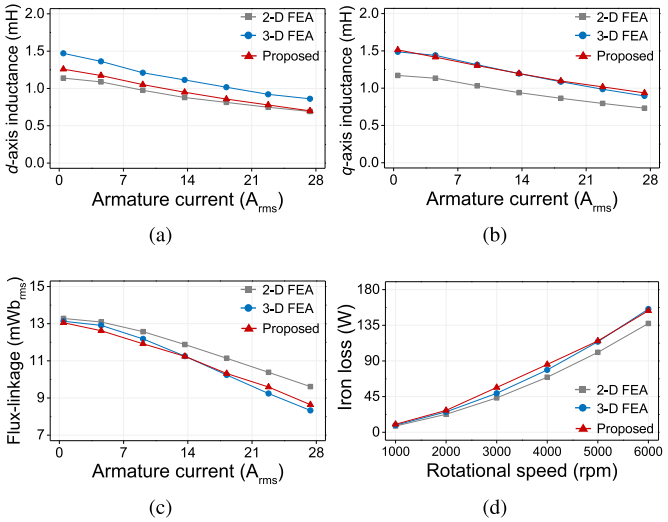

Fig. 6. Comparison of motor parameters between 2-D, 3-D FEA, and results using the proposed method. (a) d-axis inductance, (b) q-axis inductance, (c) flux-linkage, and (d) iron loss.

DNNs was converged to low values. As the domain knowledge of the source dataset was used when training target DNN with transfer learning, it can be seen that both the normalized MSEs of the training and validation datasets were converged to low values. However, in the case of DNN trained from scratch without transfer learning, it can be seen that the DNN was overfitted because the size of the target dataset was small.

Fig. 5(a)–(d) show the comparison between prediction and ground truth for the test dataset. As a result of using transfer learning, it can be seen that the regression performance on the test dataset was highly well-evaluated, and as a result of training from scratch without using transfer learning, it can be seen that the regression performance was degraded because DNN was overfitted to the training dataset. In the case of L_d and L_q, the results with transfer learning showed higher performance by about 1.5%p compared with the results without transfer learning. In the case of ψ_a and W_i, the results with transfer learning show about 3.0%p higher performance than the results without transfer learning. Therefore, high regression performance can be achieved using transfer learning with a few 3-D FEA data.

III. Sizing Results and Experimental Verification

In order to maximize the effect of axial leakage flux, the type of target motor was set as a pancake type with small α_{shape}. The peak torque, TRV, α_{shape}, and α_{split} of the target motor were set to 7.5 Nm, 116568.6 Nm/mm^3, 0.31, and 0.64, respectively. Fig. 6(a)–(d) show the comparisons of L_d, L_q, flux linkage, and iron loss between 2-D, 3-D FEA-based motor parameters and predicted results of the presented model. It can be seen that the motor parameters predicted using target DNNs according to current vector and rotational speed fit to the 3-D FEA results well except for L_d. If the number of training data increases, regression performance will be further improved and the error of L_d will also be reduced.

A specimen was fabricated and tested with a test rig as shown in Fig. 7. To consider the effect of axial leakage flux, the line current according to load torque was measured. The test was conducted at 100 rpm to exclude the effect of mechanical loss, and permanent magnet eddy current loss was neglected in characteristic calculation because it was calculated based on the predicted results using trained DNNs. Fig. 8(a) shows a trend of armature current according to load torque, and Fig. 8(b) shows an error between the simulation and experiment results. It can be seen that the simulated results by 3-D FEA had the lowest error and the predicted results using the proposed method also have higher accuracy than 2-D FEA.

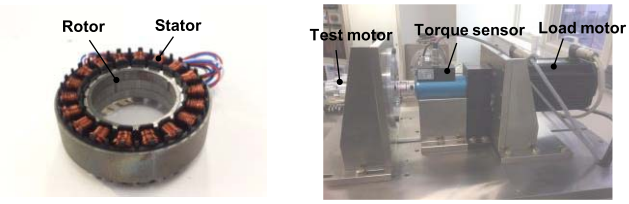

Fig. 7. Fabricated target motor and test rig.

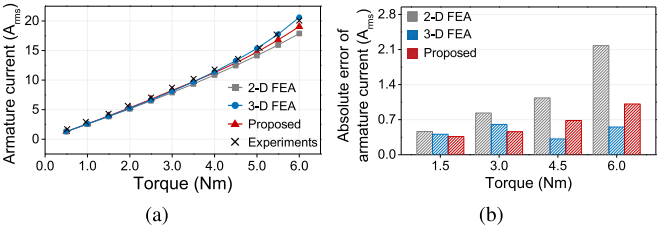

Fig. 8. Comparison of armature current according to the load torque between 2-D, 3-D FEA, results using the proposed method and experimental results. (a) Trends of armature current and (b) absolute error according to load torque.

IV. Conclusion

This article proposes a computationally efficient sizing process for PMSMs considering axial leakage flux using deep transfer learning. For the sizing process, the peak torque, TRV, shape ratio, and split ratio were considered, and 3-D FEA was

performed to consider the axial leakage flux. 3-D FEA can accurately calculate the leakage effect in the axial direction compared with 2-D FEA, but it is inefficient because of its high computational cost. Therefore, we proposed a surrogate modeling method that extremely lowers the computational cost of 3-D FEA using deep transfer learning using domain knowledge of 2-D FEA results. As a result, it was possible to predict electromagnetic characteristics of pancake-type motor which is highly affected by axial leakage flux with high accuracy by conducting small amount of 3-D FEA.

ACKNOWLEDGMENT

This work was supported by the National Research Foundation of Korea (NRF) Grant through the Korea Government (MSIT) under Grant NRF-2020R1A4A4079701.

REFERENCES

[1] S.-W. Hwang, J.-W. Chin, and M.-S. Lim, "Design process and verification of SPMSM for a wearable robot considering thermal characteristics through LPTN," *IEEE/ASME Trans. Mechatronics*, vol. 26, no. 2, pp. 1033–1042, Apr. 2021.

[2] H.-J. Kim, J.-S. Jeong, M.-H. Yoon, J.-W. Moon, and J.-P. Hong, "Simple size determination of permanent-magnet synchronous machines," *IEEE Trans. Ind. Electron.*, vol. 64, no. 10, pp. 7972–7983, Oct. 2017.

[3] K. Ramakrishnan, S. Stipetic, M. Gobbi, and G. Mastinu, "Optimal sizing of traction motors using scalable electric machine model," *IEEE Trans. Transport. Electrific.*, vol. 4, no. 1, pp. 314–321, Mar. 2017.

[4] J.-H. Park *et al.*, "Design and verification for the torque improvement of a concentrated flux-type synchronous motor for automotive applications," *IEEE Trans. Ind. Appl.*, vol. 55, no. 4, pp. 3534–3543, Jul. 2019.

[5] S. Barmada, N. Fontana, A. Formisano, D. Thomopulos, and M. Tucci, "A deep learning surrogate model for topology optimization," *IEEE Trans. Magn.*, vol. 57, no. 6, pp. 1–4, Jun. 2021.

[6] S. Doi, H. Sasaki, and H. Igarashi, "Multi-objective topology optimization of rotating machines using deep learning," *IEEE Trans. Magn.*, vol. 55, no. 6, pp. 1–5, Jun. 2019.

[7] S. Shen, M. Sadoughi, M. Li, Z. Wang, and C. Hu, "Deep convolutional neural networks with ensemble learning and transfer learning for capacity estimation of lithium-ion batteries," *Appl. Energy*, vol. 260, Feb. 2020, Art. no. 114296.

[8] S.-H. Park, E.-C. Lee, J.-C. Park, S.-W. Hwang, and M.-S. Lim, "Prediction of mechanical loss for high-power-density PMSM considering eddy current loss of PMs and conductors," *IEEE Trans. Magn.*, vol. 57, no. 2, pp. 1–5, Feb. 2021.

[9] E. Brochu, V. M. Cora, and N. de Freitas, "A tutorial on Bayesian optimization of expensive cost functions, with application to active user modeling and hierarchical reinforcement learning," 2010, *arXiv:1012.2599*.